

Pedestal effect in visual motion discrimination

William A. Simpson and Barbara A. Finsten

Department of Psychology, University of Winnipeg, 515 Portage Avenue,
Winnipeg, Manitoba, Canada R3B 2E9

Received January 17, 1995; revised manuscript received June 8, 1995; accepted June 9, 1995

Many sensory discriminations, including the discrimination of speed, obey Weber's law and thus become more difficult as the stimuli get larger. Using one-jump apparent motion stimuli, we find that the opposite can occur: displacement discrimination improves with larger jumps. This pedestal effect occurs for small jumps near and below the detection threshold. Finding a pedestal effect in motion discrimination confirms a speed energy model developed in previous experiments on the detection of jump pairs, since the pedestal effect will be observed if the visual system detects the energy of the speed waveform. Once the size of the jumps becomes large enough, the discriminability declines, indicating masking. Masking is just the detectability counterpart of Weber's law; it is not predicted from energy detection. The pedestal effect shows the presence of a squaring nonlinearity for small speed signals, and masking indicates linear transduction for large signals. A half-wave rectifier, when presented with Gaussian noise, behaves this way. The speed energy model can be seen as an approximation, valid for small signals, to a model that includes half-wave rectification. © 1995 Optical Society of America

1. INTRODUCTION

Although many studies of visual speed discrimination have been published,¹⁻⁹ none has examined the discrimination of very slow speeds near and below the detection threshold. The detection threshold is the speed required for reliable discrimination of a stationary stimulus and a moving stimulus. A model of motion sensing developed by Simpson¹⁰ leads us to believe that peculiar things will happen to speed discrimination when the standard is very small.

In a previous set of experiments,¹⁰ Simpson measured the displacement detection threshold for pairs of jumps. Since a jump is a motion impulse, the temporal properties of the motion system can be studied with the two-impulse technique originally used by Rashbass¹¹ for pairs of light flashes. By presenting pairs of jumps of various sizes to the left and right, separated by various delays, it was possible to examine the motion system's temporal impulse response (albeit indirectly). A simple model accounted for the data. The model indicates that the speed signal in the world, $v(t)$, is passed through a linear filter [convoluted with the temporal impulse response $h(t)$], squared, and integrated over some rather long duration τ :

$$\int_0^\tau [v(t) * h(t)]^2 dt. \quad (1)$$

Since squaring and integrating a signal computes its energy, this can be called a speed energy model (not to be confused with Adelson and Bergen's¹² motion energy). Gaussian noise is added, limiting performance. A schematic diagram of the model is shown in Fig. 1.

An energy detector shows peculiar behavior for discrimination between a standard stimulus and a comparison stimulus when the size of the standard is small. In the speed energy model the discriminability of stimuli depends on the difference in their speed energies. The stimuli to be compared are two jumps. The speed of a

jump is $a\delta(t)$, where a is the displacement or size of the jump (in arcmin) and $\delta(t)$ is the Dirac delta function (in units of s^{-1}). If we call the displacement for the standard a and the displacement for the comparison $a + \Delta a$, then the discrimination is between the speed waveforms $v_s(t)$ and $v_c(t)$:

$$v_s(t) = a\delta(t), \quad (2)$$

$$v_c(t) = (a + \Delta a)\delta(t). \quad (3)$$

(Note that since the unit for displacement is arcmin and the unit of the delta function is s^{-1} , the unit for speed is min s^{-1} . Therefore one may describe the task equally correctly as displacement discrimination, with unit min, or as speed discrimination, with unit min s^{-1} .)

The discrimination is based on the difference of the energies of $v_s(t)$ and $v_c(t)$. Let us compute these in turn by substituting $v_s(t)$ and $v_c(t)$ for $v(t)$ in Eq. (1). The speed energy E_s of the standard is

$$\begin{aligned} E_s &= \int_0^\tau [a\delta(t) * h(t)]^2 dt = \int_0^\tau [ah(t)]^2 dt \\ &= a^2 \int_0^\tau h^2(t) dt. \end{aligned}$$

Let

$$\int_0^\tau h^2(t) dt = 1.$$

Then

$$E_s = a^2. \quad (4)$$

For the comparison,

$$\begin{aligned} E_c &= \int_0^\tau [(a + \Delta a)\delta(t) * h(t)]^2 dt = \int_0^\tau [(a + \Delta a)h(t)]^2 dt \\ &= (a + \Delta a)^2 \int_0^\tau h^2(t) dt. \end{aligned}$$

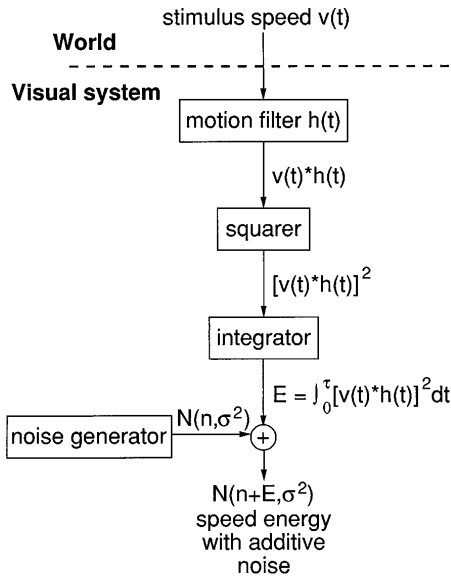


Fig. 1. Flow chart of speed energy model. The stimulus speed in the world $v(t)$ is filtered, squared, and integrated. The filtering stage corresponds to speed recovery [recall that $v(t)$ is the stimulus] in the brain. Normal noise is added to the speed energy, thus limiting performance.

Again setting the energy of the impulse response to 1, we get

$$E_c = (a + \Delta a)^2. \quad (5)$$

Gaussian noise with mean n and variance σ^2 is added to E_s and E_c . The observer therefore has to discriminate between the two Gaussian processes $N(n + E_s, \sigma^2)$ and $N(n + E_c, \sigma^2)$. The measure of discriminability d' is defined¹³ as the difference of the means of the Gaussian processes divided by their standard deviation:

$$\begin{aligned} d' &= \frac{(n + E_c) - (n + E_s)}{\sigma} = \frac{E_c - E_s}{\sigma} = \frac{(a + \Delta a)^2 - a^2}{\sigma} \\ &= \frac{2a\Delta a + \Delta a^2}{\sigma}. \end{aligned} \quad (6)$$

When the difference in displacements (Δa) is fixed, detectability will rise linearly as the standard displacement (a) increases.

The speed energy model, then, predicts that it will become easier to discriminate two jumps as the size of the standard jump increases. This is the opposite of what Weber's law would lead one to predict. Weber's law can be stated as

$$\Delta a_{\text{thresh}} = \sigma a + \sigma_0, \quad (7)$$

where Δa_{thresh} is the difference threshold, σ is the standard deviation of the Gaussian noise in the motion system, and σ_0 is the standard deviation of this noise at absolute threshold (i.e., when $a = 0$). Weber's law states that the difference threshold increases linearly with the size of the standard. We do not measure Δa_{thresh} but instead measure d' for a fixed Δa . In terms of d' we have

$$d' = \frac{\Delta a}{\sigma a + \sigma_0}, \quad (8)$$

which the reader can verify by setting d' to 1, its value

at threshold, giving Eq. (7). The behavior predicted by Eq. (8) will be called masking. We take this term from the auditory literature. Masking means that for a fixed difference in stimuli, d' declines as the size of the standard increases. Weber's law and masking go hand in hand and refer to the same basic phenomenon measured with thresholds in the first case and d' in the second.

The speed energy model predicts the opposite of Weber's law and masking: instead of getting harder it should become easier to discriminate the stimuli as the size of the standard grows. We expect d' to increase as the size of the standard increases. This departure from masking predicted by the speed energy model is called the pedestal effect. (Note that sometimes the term pedestal effect is used to denote what we would call negative masking: the difference threshold declines as the standard increases.) The name comes from looking at the discrimination task as being one of detecting an increment placed on a background or pedestal. This is not a strictly correct way to look at discrimination in our experiment: the comparison is not formed by superimposing an increment on a steady background but is instead presented separately from the standard, and so our task is difference discrimination, not increment detection (for the importance of this distinction see Laming¹⁴). The pedestal effect has been observed before for luminance discrimination^{15,16} and for discrimination of the amplitude of auditory waveforms.¹⁷ In both cases the pedestal effect was found when the standard was near and below the detection threshold.

The speed energy model, derived to describe the results of two-jump temporal summation experiments, predicts that a pedestal effect should be found for jump discrimination. We test that prediction by measuring displacement discrimination as a function of the size of the standard.

2. METHOD

A. Subjects

The authors, WS and BF, both corrected myopes, served as subjects.

B. Stimuli

1. Main Experiment

The stimulus on each trial was a random-square display that jumped to the right by a small or large amount. The difference in the displacements was fixed at 1.16 arcmin; the standard took on the values indicated in Fig. 3 below. The comparison was therefore 1.16 arcmin plus the standard displacement. The motion sequence was a single jump consisting of two frames, each 16.67 ms long, and presented with no interstimulus interval. Conventional wraparound was used. Each frame contained 100 randomly positioned bright (150 cd/m²) 4.46-arcmin squares on a dark background (13 cd/m²). The squares filled a 2.02 × 1.27 deg area. The sequences were generated on an Amiga computer and displayed on a P31 phosphor monitor. A veiling incandescent light was used to mask phosphor trails. Viewing was monocular from a chin and forehead rest. Observers fixated on a small LED 0.73 deg to the right of the top-right corner of the display.

2. Control Experiment

In the main experiment there are differences between the standard and the comparison besides the size of their displacements (or speeds). For example, a time average of the two motion sequences would yield streaks of differing lengths. Thus a purely spatial mechanism, rather than a motion mechanism, could perform the discrimination. The detailed pattern of flicker is different for standard and comparison as well, and thus a purely temporal mechanism could perform the discrimination. Since a spatiotemporal stimulus (motion) is being presented it seems unlikely that the visual system would use only part of the information given. Still, it would be nice to have some assurance that a motion mechanism is really being used.

Simpson¹⁰ described a stimulus pair differing in speed that contains the same flicker and time-averaged dot length, forcing the visual system to use motion. In that paper a detection task was used, so the stimulus must be slightly modified here. Both standard and comparison contains dots moving with the same absolute size of displacement. The difference is in the proportions of dots moving left and right (see Fig. 2). The standard and comparison therefore differ in the space-averaged speed or displacement. For example, if the standard has 60% of its dots moving right with displacement a and 40% moving left with displacement $-a$, and the comparison has 70% of its dots moving right and 30% moving left, the space-averaged displacements are $0.6a + 0.4(-a) = 0.2a$ for the standard and $0.7a + 0.3(-a) = 0.4a$ for

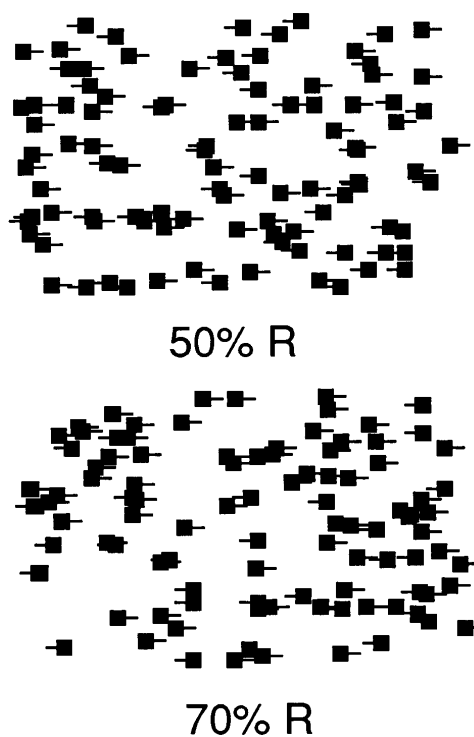


Fig. 2. We manipulated the space-averaged speed in the control experiment by varying the percentage of squares moving right (the rest moving left). Two example stimuli are shown; the line segments point in the direction of motion. This figure illustrates the standard stimulus (50%) and the comparison stimulus (70%) for a 20% difference in the percentage of dots moving right.

the comparison. The difference in the energy of these space-averaged speeds is computed by the visual system. Watamaniuk and Duchon¹⁸ and Smith *et al.*¹⁹ have shown that motion signals are space-averaged by the visual system, although they did not use dots moving in opposite directions. Since the moving and stationary stimuli are alike in every way except for the space-averaged speed, it is impossible to discriminate them using nonmotion cues such as the time-averaged lengths of the dots or their flicker.

Most of the stimulus details were as described in the main experiment, except that now the standard and comparison differed in proportions of rightward-moving squares (rather than in displacement size). The displacement was 3.88 arcmin. The comparison had more squares moving to the right than did the standard. For BF the comparison always had 20% more rightward-moving dots and for WS the comparison had 10% more rightward-moving dots. Several percentages of rightward-moving dots were used for the standard (BF: 50%, 60%, 70%, 75%, 80%; WS: 50%, 60%, 70%, 80%, 90%). In terms of the average speeds, the task was to detect a fixed difference in average speed as a function of the average speed of the standard.

C. Procedure

In the main experiment each trial contained either the standard or the comparison displacement. Each standard was run in a separate block of trials. The ordering of standards across blocks was random. In a block of trials the standard and comparison were presented in random order with equal probability. The observers used a 6-point scale to rate their confidence that the comparison had been presented.^{20,21} A rating of 1 indicated high confidence that the comparison (faster) stimulus had been presented, a rating of 6 indicated low confidence that the comparison had been presented, and intermediate ratings indicated intermediate levels of confidence. For observer WS the receiver operating characteristic (ROC) for all the standards were based on 200 trials except for the standard displacement of 3.88 arcmin, which was based on 400 trials. For observer BF the number of trials for each standard displacement was 400 (0.78, 1.16, 1.94 arcmin), 450 (0.39 arcmin), and 600 (1.55, 2.91, and 3.88 arcmin).

We used the confidence rating procedure for several reasons. First, the ROC is an important psychophysical function to obtain and, to our knowledge, no ROC's for speed (displacement) discrimination have been published. Indeed, Laming²² comments that very few ROC's for difference discrimination in *any* sensory modality have been published (he cites only three). Second, by obtaining the ROC's we can assess the validity of the equal-variance Gaussian model of Fig. 1. Finally, compared with other methods, the rating method gives more information, is more efficient, or both. Compared with yes-no or two-interval forced-choice (2IFC), the rating method is more informative since it gives the ROC. Compared with 2IFC, the rating method uses the observer's time more efficiently, since he or she views half the number of stimuli in the same number of trials. Spatial forced choice uses the same number of stimuli as the rating method, but it creates a spatial step in speed across the display instead of the uniform vector field

that we desired. Readers unfamiliar with signal detection theory may think that forced-choice methods are better since they are unbiased. This is a misconception on two counts. First, there is no guarantee in forced-choice methods that responses will be unbiased²³ (although often it does turn out that way). Second, the existence of a nonzero criterion (bias), even one that is changing, is not at all problematic, since the criterion and detectability are independent and uncorrelated.²⁴ That is, the detectability is unaffected by the bias.

In the control experiment both standard and comparison were presented in random order on every trial. The observers picked the interval containing the comparison (2IFC). A hit was defined as the response "first" when the comparison was in the first interval; a false alarm was defined as the response "first" when the comparison was in the second interval. For the 2IFC case, d' is $Z(\text{hit}) - Z(\text{false alarm})/\sqrt{2}$, where $Z(\cdot)$ indicates the inverse normal integral. In each block of 50 trials a fixed standard and comparison were used. The order of the standards (across blocks) was random. Each measured d' was based on at least 200 trials.

Using the same stimuli as those used in the main experiment, we measured the threshold displacement for detecting a jump. The task was to discriminate a moving display from a stationary display. One or the other was presented on each trial. d' was measured for each of several displacements (5 for WS, 6 for BF). A minimum of 200 trials was run for each d' . A curve was fitted to the resulting d' 's. From this curve the displacement required to yield a d' of 1 was determined. This is the absolute threshold or detection threshold.

3. RESULTS AND DISCUSSION

ROC's for displacement discrimination were calculated from the rating data in the conventional way.^{20,21} For each pair of standard and comparison, the frequency of each rating was tabulated. Dividing by the number of trials for each stimulus converted the counts to proportions. Then the proportions were cumulated from left (rating of 1) to right (rating of 6). The inverse normal integral of each proportion was then found (this is not strictly a necessary step, but we wanted to plot the ROC on Z - Z coordinates). The ROC is simply the plot of each pair of Z 's (false alarm-standard hit comparison) for each rating. In this way an ROC of 5 points was obtained from 6-point rating scale data.

The ROC's, plotted on inverse normal integral x and y axes, are shown in Fig. 3. The figure shows 7 ROC's for each observer; the difference in displacements was fixed and 7 different standard displacements were used.

According to the speed energy model, the input speed is filtered, squared, and integrated. We earlier supposed that the standard and comparison speed energies are represented in the brain as the means of Gaussian processes having equal variances [see Eq. (6) and Fig. 1]. If this supposition is correct, the ROC data points should fall on straight lines in Z - Z coordinates, and these lines should be parallel to the $Z(\text{hit}) = Z(\text{false alarm})$ diagonal.

Both observers' ROC's are well fit by straight lines. The slopes of the ROC's, however, are not necessarily 1 (see Table 1). The obtained slopes for the ROC's of BF

ranged from 0.93 to 1.17 so her data are consistent with an equal-variance-Gaussians prediction. For WS the slopes ranged from 0.64 to 1.06. The shallow-slope data deviate from an equal-variance-Gaussian prediction. For the smaller standard stimuli, WS's data are described by Gaussians with unequal variance: the comparison distribution has a variance approximately 1.25 times as big as the standard's variance (the ratio of variances is given by the reciprocal of the ROC slope). This is not a huge departure from an equal-variance-Gaussian model.

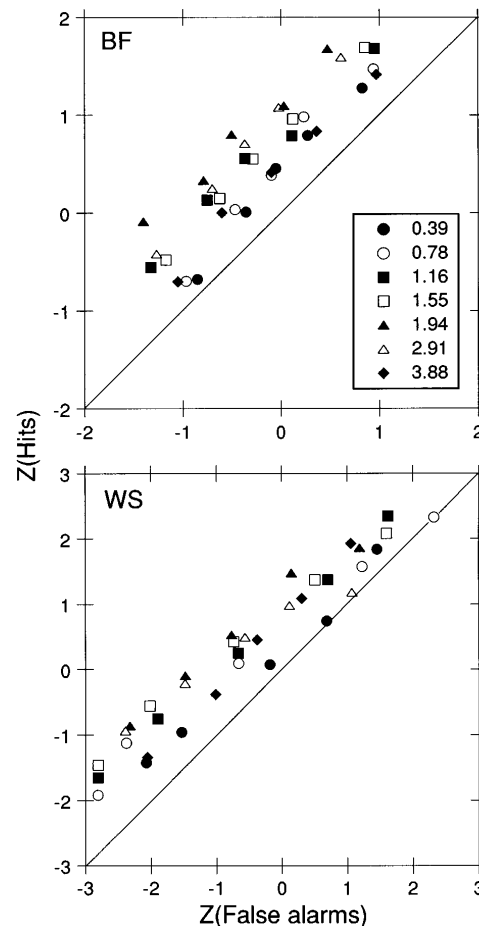


Fig. 3. Receiver operating characteristics on Z - Z coordinates (Z is the inverse normal integral) for discrimination of the displacement in a two-frame apparent motion sequence. On each trial either the standard or the comparison (larger) displacement was presented with equal probability, and the observers (BF and WS) used a 6-point scale to rate their confidence that the comparison had been presented. The difference in the displacements was fixed at 1.16 arcmin; the standard took on the displacement values (in arcmin) indicated in the legend.

Table 1. Slopes of ROC's

Standard Displacement (arcmin)	Slope	
	BF	WS
0.39	1.17	0.88
0.78	1.15	0.79
1.16	0.95	0.88
1.55	1.07	0.79
1.94	0.93	0.80
2.91	1.08	0.64
3.88	1.01	1.06

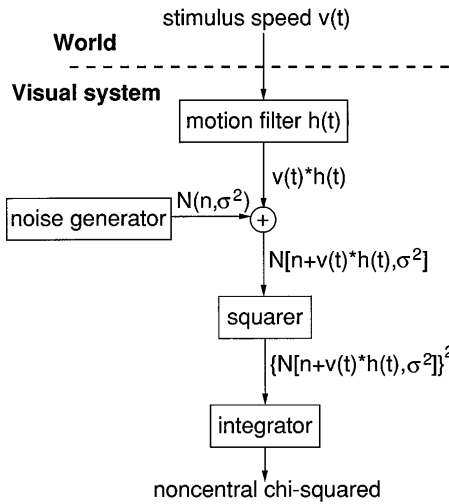


Fig. 4. Alternative view of how noise enters the speed energy computation. After speed recovery in the brain (motion filtering), normal noise is added. The normal process is then squared and integrated. The result is a noncentral chi-squared variable with the noncentrality parameter equal to the speed energy.

We originally assumed that the speed energies of standard and comparison were represented by the means of equal-variance-Gaussian distributions. We could have assumed instead that the speeds of the standard and comparison stimuli as extracted by a motion sensor were equal-variance-Gaussian processes (see Fig. 4). Internal Gaussian white noise is superimposed on both, and this limits performance. When the Gaussian process for (standard + noise) or (comparison + noise) is squared and integrated, the result is a pair of noncentral chi-squared processes²⁵ whose noncentrality parameter is the speed energy.

The prediction from this treatment is that the ROC's should have slopes that are less than 1.0, especially for small standard stimuli. As the size of the standard increases, the slope should approach 1.0 (see Green and Swets²⁵). This seems to describe the ROC's obtained from WS. In any case, as mentioned earlier, the departure of the data from the simple equal variance Gaussian model is not very large.

The criterion is not important for assessing any model under discussion, but we note in passing that the consistency of each observer's criterion placement can be seen in Fig. 3. If each criterion stays completely fixed, all the points in the ROC should fall on lines with slope -1; that is, as the detectability increases, each point moves at right angles away from the $Z(\text{hit}) = Z(\text{false alarm})$ diagonal.²⁶ The data from BF show remarkable consistency in criterion placement. The data from WS show some criterion drift. BF had more practice with the task, and her data points are based on more trials; this would account for her higher criterion stability. Criterion drift is no problem, since detectability and criterion are independent.

The main prediction for this experiment was about how the discriminability of the standard and comparison should vary as the size of the standard increases. We thus need to compute a measure of discriminability from the ROC's. As we have seen, the ROC's do not necessarily have slopes of 1.0. Since d' assumes an ROC slope of 1.0, d' is not the best choice. Several ways to cope with

this situation exist. One can use the absolute value of the ROC's x intercept, measuring d' in the units of the standard deviation of the standard. One can use the y intercept of the ROC, measuring d' in the units of the standard deviation of the comparison. Finally, one can attempt to combine the two standard deviations somehow, giving a value of d' intermediate between the x intercept and y intercept d' 's. The index that we use, d_a , finds the difference between the means of the two random variables (standard and comparison) in units of the root-mean-square standard deviation.^{27,28} The two standard deviations are squared, the mean is found, and the square root is taken. Once the slope and the y intercept of the ROC in $Z-Z$ coordinates are known, d_a can be calculated:

$$d_a = y \text{ intercept} \sqrt{2/(1 + \text{slope}^2)}.$$

Figure 5 shows d_a plotted as a function of the standard displacement. The most important feature of this figure is that for small standards a fixed difference in speeds (or displacements) becomes more detectable as the standard increases in size. This is the opposite of the pattern that masking (the counterpart of Weber's law) would predict. It is the pedestal effect, as predicted from the speed energy model. As the standard grows larger, eventually the detectability of the difference declines, showing masking.

The data show a linear increase in detectability as the standard increases in size, as predicted by the energy model [Eq. (6)]. This pedestal effect is shown for standards that are near detection threshold and below. The detection threshold was measured in a separate experiment to be 1.56 arcmin for BF and 1.44 arcmin for WS. We mentioned above that a pedestal effect has been found for luminance and auditory amplitude discrimination.¹⁵⁻¹⁷ In these other cases, as here, the pedestal effect occurs near and below detection threshold.

Once the standard displacement becomes large enough the detectability begins to decline, indicating masking [Eq. (8)]. Masking in speed or displacement discrimination has not, to our knowledge, been demonstrated before, but its existence is expected from Weber's law, which is known to hold for multijump displays at higher speeds.^{5,6}

The data in Fig. 5 are fitted by the piecewise function

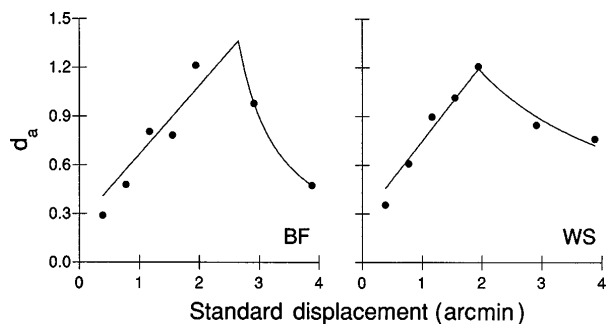


Fig. 5. Detectability of the displacement difference as a function of the size of the standard displacement for each observer. The detectability measure d_a was computed from the ROC's of Fig. 2. The curve is a least-squares fit of Eq. (9), which is composed of a pedestal effect section at low values of the standard and a masking section at higher values.

$$d_a = (a < b) \frac{2a\Delta a + \Delta a^2}{(2b + \Delta a)(\sigma b + \sigma_0)} + (a \geq b) \frac{\Delta a}{\sigma a + \sigma_0}, \tag{9}$$

where b is the break point dividing pedestal effect and masking behavior and $(a < b)$ and $(a \geq b)$ are Boolean. This function pieces together the pedestal effect for small standard speeds (below the break point) and masking for higher speeds (above the break point). It can be seen that the fit of Eq. (9) to the data is satisfactory.

The pedestal effect was also found in the control experiment, which used a different procedure and different stimuli. The control was run to counter the view²⁹ that observers may discriminate speed or displacement by using only the spatial or only the temporal aspect of the display. We designed a control stimulus that would defeat such nonmotion mechanisms. The standard and the comparison stimuli contained the same number of squares moving the same distance. They differed in the proportions of these squares moving to the right and the left (see Fig. 2). Therefore the standard and comparison stimuli differed in space-averaged speed. Such statistical stimuli cannot be discriminated with simple time-averaged dot length or flicker cues. The experiment consisted in presenting a fixed difference in the proportion of rightward-moving squares in the standard and comparison at several levels of the standard proportion of rightward-moving squares. The space-averaged displacement of the standard takes on several values while the space-averaged difference in displacements is fixed.

We have described the statistical stimulus in terms of its space-averaged speed. Will the motion system do such a space-average? Others have found evidence for space-averaging of dot speeds. However, in our stimulus the dot speeds are opposite in sign, and no other authors have studied motion detection or discrimination with dots moving in opposite directions. Perhaps it is unreasonable to think that speed-averaging takes place regardless of motion direction. Suppose, for example, that instead of space-averaging, the speeds of the dots moving rightward are summed and the (unsigned) speeds of the leftward moving dots are summed. The difference of these two sums is taken. The stimulus with the larger left-right difference is the comparison. This alternative mechanism is essentially the same as space-averaging: space-averaging just divides the left-right difference by the number of dots. In summary, we talk about the stimulus in terms of its space-average speed because prior results showed such space-averaging to exist and because any sensible discrimination method is essentially the same as finding the space average.

We assume that space averaging of the speed signal precedes the speed energy computation; that is, before squaring and temporal integration, the speeds over the whole display are recovered. In the process of recovery the speeds are spatially and temporally filtered. The spatial filtering is low pass; hence the speeds are space averaged. In the display used here, we can no longer ignore the spatial aspect of the speeds, since they are not uniform over the whole display. The speed signal $v(x, y, t)$ is

$$v(x, y, t) = [2 \text{Bernoulli}(p) - 1]a\delta(t), \tag{10}$$

where $\text{Bernoulli}(p)$ denotes a Bernoulli random variable and p is the probability that a square moves to the right. The speed energy is

$$E = \int_0^\tau \int_0^\sigma [v(x, y, t) * h(x, y, t)]^2 dx dt. \tag{11}$$

Now the speed is a function of space as well as time, and the same is true for the motion filter. The motion filter does the space averaging. This space averaging could happen at the same time as speed extraction, or the speeds could be first extracted at each retinal location and spatially averaged subsequently. Either interpretation of Eq. (11) can be made, since $v(x, y, t) * h(x, y, t) = [v(x, y, t) * h(t)] * h(x, y)$.

The average speed is

$$\bar{a} = ap - a(1 - p), \tag{12}$$

where p is the proportion of rightward-moving squares. The difference in average speeds is

$$\begin{aligned} \Delta\bar{a} &= \{a(p + \Delta p) - a[1 - (p + \Delta p)]\} - [ap - a(1 - p)] \\ &= 2a\Delta p, \end{aligned} \tag{13}$$

where Δp is the difference in proportions of rightward-moving squares. The predictions for the statistical stimulus are the same as in the main experiment except that \bar{a} and $\Delta\bar{a}$ are substituted for a and Δa in Eqs. (6), (8), and (9).

As in the first experiment, the data (Fig. 6) show a pedestal effect for small values of the standard and masking for larger values. In the pedestal effect regime, d' increases linearly with the average speed (proportion of rightward-moving squares) as predicted by Eq. (6). Overall the d' function can be fitted with the tent-shaped function given by Eq. (9). The fit is satisfactory.

We find a similar pattern of results in Figs. 5 and 6. By using a statistical stimulus in the control experiment, we rule out the idea that the data reveal the workings of a nonmotion mechanism. Moreover, the similarity of the data obtained with the traditional and the statistical stimuli suggests that both tap a motion mechanism.

After these experiments had been conducted, our attention was drawn to an earlier displacement-identification experiment by Levi *et al.*³⁰ The experimental data are

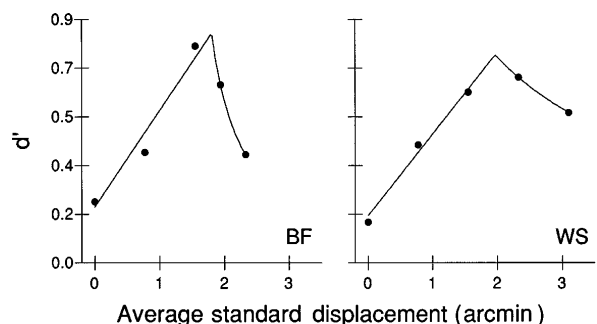


Fig. 6. Data from the control experiment in which the observer discriminated between displays with different proportions of rightward-moving squares. The detectability of the space-averaged displacement difference, d' , is plotted as a function of the space-averaged speed of the standard. This percentage determines the space-averaged displacement.

presented in their Fig. 7; we give a different treatment of these data. The amblyopic subject was presented with a grating of bright lines that jumped 0, 1, 2, or 3 units to the left or right (the exact size of these jumps is uncertain, though probably on the order of half an arcmin). The task was to say which displacement had been presented: there were seven ratings and seven stimuli. Note that this is an identification experiment, quite different from the first experiment presented here, which is a discrimination experiment. Superficially the two experiments are similar in that both used ratings, but the discrimination experiment had only two stimuli in each block of trials, the standard and the comparison, and the different ratings did not categorize the size of the jump but instead expressed confidence that it was the standard or comparison.

Each ROC in Fig. 7 is based on a pair of jumps that differ in size by one unit. The standard is $-3, -2, -1, 0, 1, \text{ or } 2$, and the comparison is one unit larger. The ROC is computed in a way similar to that described earlier.³¹ Inspection of the ROC's reveals two facts. First, as with our data (Fig. 3), the ROC's are well described by lines of unit slope on Z - Z axes. This is what the equal-variance-Gaussian model would lead us to expect. Second, a pedestal effect is apparent. This is made clearer in Fig. 8, which plots d_a as a function of the size of the standard. Detectability is lower for stimulus pairs 0 versus -1 and 0 versus 1 (standards of -1 and 0, respectively) than it is for pairs of larger jumps to the left or right. This is the pedestal effect. At the largest standard, d_a does not rise. If a larger standard had been presented, we probably would have observed masking: d_a would start to decline.

A pedestal effect was found in the main experiment, the control experiment, and the study by Levi *et al.*³⁰ This is predicted by the speed energy model. However, masking was found once the standard became large enough. Masking is not predicted from an energy detector, though it can be obtained with modifications.²⁵ A full account of the data would be able to predict both the pedestal effect and masking.

Laming³² has proposed the only model we know of that predicts both the pedestal effect and masking. The model is complicated and was originally formulated in the domain of luminance. We present a simplified model that bears a loose resemblance to the Laming model. The input velocity waveform is low-pass filtered. Gaussian noise is added to it. The noisy waveform is half-wave rectified and then integrated for some duration. This model is similar to the speed energy model shown in Fig. 4, with a half-wave rectifier replacing the squarer. The substitution of a half-wave rectifier is the key to producing both the pedestal effect for small stimuli and masking for larger stimuli. When the input is Gaussian noise, Laming has shown that the half-wave rectifier acts as a squarer for small signals and as a linear transducer for large signals. Thus the model behaves like the energy model for small stimuli, and a pedestal effect is seen. At large stimulus values the approximate mean output from the integrator is strictly proportional to the stimulus amplitude. This is necessary to produce masking, but it is not enough. The standard deviation of the integrator output must be proportional to the size of the stimulus.

(One way to get such behavior is to add the several stages that we have omitted from Laming's full model.) At large stimulus values the linear transduction of the stimulus combined with the increasing variance will give rise to masking.

The transition from pedestal effect to masking is seen at a level of the standard just higher than detection threshold. This transition happens when the size of the signal goes from small to large. Small stimuli are subject to squaring (approximately), and large ones are transmitted in strict linear proportion. If we interpret a small signal as being below detection threshold and a large one as being above detection threshold, the observed transition from pedestal effect to masking is compatible with the half-wave-rectifier model.

The predictions of the half-wave-rectifier model on the shape of the ROC for a difference discrimination (Figs. 3 and 7) are also consistent with the data. The input to the half-wave rectifier is Gaussian. For small signals the half-wave rectifier acts like a squarer. After squaring and integration the output is distributed as noncentral chi-squared. Since the noncentral chi-squared variance for the standard is smaller than that for

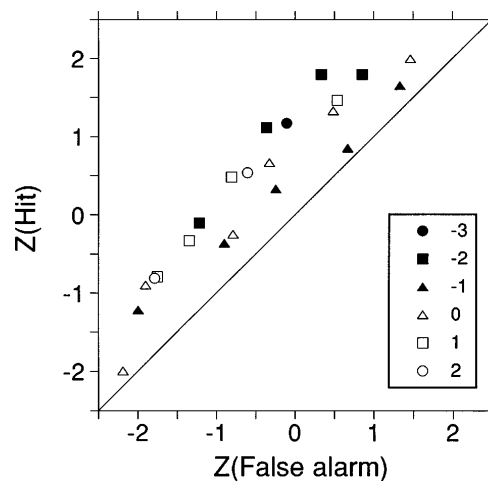


Fig. 7. ROC's computed from data supplied by D. Levi.³⁰ The task was to identify, with a 7-point rating, which of 7 different displacements was presented. The size of the standard displacement in arbitrary units is shown in the legend. The difference in displacements is fixed at one unit. Each ROC signifies one pair of standard and comparison.

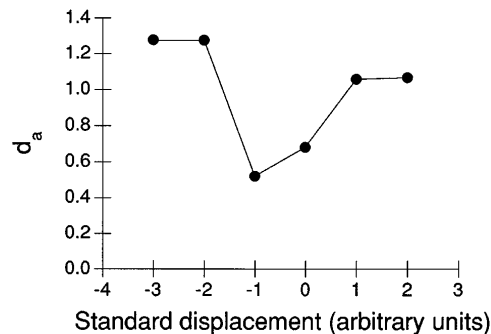


Fig. 8. Discriminability d_a computed from each ROC in Fig. 7, as a function of the standard displacement. The discriminability for the larger standards (jumps to the left or right) is higher than for standards near zero. This is the pedestal effect.

the comparison stimulus, the result for small signals is an ROC with slope less than 1 on Z - Z coordinates.³³ For large signals we have linear transduction, so after integration, the output is still Gaussian. The variance does not depend on the size of the stimulus (whether standard or comparison). With equal-variance Gaussians we get an ROC with slope 1 on Z - Z coordinates. This pattern—ROC slopes less than 1 for small standards but becoming closer to 1 for large standards—is shown by observer WS. For observer BF the slopes seem to stay near 1 for all standards. Perhaps this means that the half-wave-rectifier model is wrong, but we caution that ROC slopes are more variable than are detectabilities.

If the half-wave rectifier model is correct, the speed energy model is only an approximation that works for small signals near and below threshold. For these sorts of stimulus the rectifier acts like a squarer, and so the two models behave the same way. At higher signal levels the half-wave rectifier behaves linearly.

4. CONCLUSIONS

We have shown the pedestal effect, using two very different sorts of moving stimulus. The pedestal effect is predicted from a model that posits detection of speed energy. This model was first proposed to explain results of experiments on detection of pairs of jumps¹⁰; the convergence of findings from these very different experiments constitutes strong support for the model. The speed energy appears to be computed only for small stimuli, however. Once the stimuli become large enough, we find masking, which is not predicted by the speed energy model. The overall pattern of results—speed energy detection at low signal levels and linear transduction at higher levels—is consistent with a half-wave-rectifier model. We view the speed energy model as an approximation to the half-wave-rectifier model that is valid for small stimuli.

The half-wave-rectifier model has several elements. First, the velocity waveform is temporally low-pass filtered (by the mechanism that extracts the velocity from the spatiotemporal luminance waveform falling on the retina). Gaussian noise is added. The filtered signal with added noise is then passed through a half-wave rectifier. The output of the rectifier is integrated. These model elements are realistic, given what we know about motion cells. It seems quite plausible that MT or V1 complex cells should produce an output analogous to a low-pass filtered speed, although we are not aware of any electrophysiological studies that have examined the temporal impulse response or the frequency response of motion cells to jumping or oscillating stimuli. Any neuron's firing rate is noisy. Directionally selective cells^{34–36} are half-wave rectifiers of the speed signal; that is, they respond only to one of two opposite directions (positive and negative) of motion along an axis. The output of a directionally selective cell can be integrated, implementing the model.

The motion system acts like an energy detector for small signals. Evidence for energy detection has been found in other domains, including audition³⁷ and luminance.¹¹ Among the support for energy detection is the pedestal effect, which has been found in the discrimination of auditory intensity¹⁷ and luminance.^{15,16}

Energy detection is an efficient approach to take if the signal has an unknown form³⁸ or if the signal is a pulse of unknown phase.³⁹ However, in the present motion experiments the form of the signal was known to be an impulse and the phase of the signal was known (it was delivered a fixed time after a keypress). There were only two stimuli in a block of trials: impulses of known amplitudes. Why then energy detection? There are at least two possible interpretations. First, there may be a hard-wired simple mechanism (the half-wave-rectifier model) that computes energy and cannot use any information about the form of the signal. This nonoptimal mechanism is simple and will perform reasonably well. A second possibility is that the information about the signal waveform can be used in principle (in a cross-correlator mechanism, for example), but even though there should be no uncertainty about the form of the signal, uncertainty is introduced at some level of processing in the brain.^{40,41} In any case, by using energy, the observer acts as though he or she is ignorant or uncertain about the form of the signal to be detected.

ACKNOWLEDGMENTS

This work was supported by an operating grant from the Natural Science and Engineering Research Council (NSERC) to W. A. Simpson. B. A. Finsten was supported by an NSERC Undergraduate Research Award. We thank D. Laming, Bruce Schneider, and Shin'ya Nishida for their helpful comments.

Address all correspondence to W. A. Simpson, e-mail address wsimpson@uwinnipeg.ca.

REFERENCES

1. B. B. Brandalise and R. M. Gottsdanker, "The difference threshold of the magnitude of visual velocity," *J. Exp. Psychol.* **57**, 83–88 (1959).
2. R. H. Brown, "Visual sensitivity to differences in velocity," *Psychol. Bull.* **58**, 89–103 (1961).
3. B. De Bruyn and G. A. Orban, "Human velocity and direction discrimination measured with random dot patterns," *Vision Res.* **28**, 1323–1335 (1988).
4. W. E. Hick, "The threshold for sudden changes in the velocity of a seen object," *Q. J. Exp. Psychol.* **2**, 33–41 (1950).
5. F. J. Mandriotta, D. E. Mintz, and J. M. Notterman, "Visual velocity discrimination: effects of spatial and temporal cues," *Science* **138**, 437–438 (1962).
6. S. P. McKee, "A local mechanism for differential velocity detection," *Vision Res.* **21**, 491–500 (1981).
7. S. P. McKee, G. H. Silverman, and K. Nakayama, "Precise velocity discrimination despite random variations in temporal frequency and contrast," *Vision Res.* **26**, 609–619 (1986).
8. J. M. Notterman and D. E. Page, "Weber's law and the difference threshold for the velocity of a seen object," *Science* **126**, 652–653 (1957).
9. K. Turano and A. Pantle, "On the mechanism that encodes the movement of contrast variations: velocity discrimination," *Vision Res.* **29**, 207–221 (1989).
10. W. A. Simpson, "Temporal summation of visual motion," *Vision Res.* **34**, 2547–2559 (1994).
11. C. Rashbass, "The visibility of transient changes of luminance," *J. Physiol.* **210**, 165–186 (1970).
12. E. H. Adelson and J. Bergen, "Spatiotemporal energy models for the perception of motion," *J. Opt. Soc. Am. A* **2**, 284–299 (1985).
13. D. M. Green and J. A. Swets, *Signal Detection Theory and Psychophysics* (Peninsula, Los Altos, Calif., 1988), pp. 60–61.

14. D. Laming, *Sensory Analysis* (Academic, Toronto, 1986), pp. 67–69.
15. B. Leshowitz, H. B. Taub, and D. H. Raab, “Visual detection of signals in the presence of continuous and pulsed backgrounds,” *Percept. Psychophys.* **4**, 207–213 (1968).
16. J. Nachmias and E. C. Kocher, “Visual detection and discrimination of luminance increments,” *J. Opt. Soc. Am.* **60**, 382–389 (1970).
17. S. M. Pfafflin and M. V. Mathews, “Energy-detection model for monaural auditory detection,” *J. Acoust. Soc. Am.* **34**, 1842–1853 (1962).
18. S. N. J. Watamaniuk and A. Duchon, “The human visual system averages speed information,” *Vision Res.* **32**, 931–941 (1992).
19. A. T. Smith, R. J. Snowden, and A. B. Milne, “Is global motion really based on spatial integration of local motion signals?” *Vision Res.* **34**, 2425–2430 (1994).
20. Ref. 13, pp. 101–106.
21. N. A. MacMillian and C. D. Creelman, *Detection Theory: A User's Guide* (Cambridge U. Press, New York, 1988), pp. 58–77.
22. Ref. 14, p. 78.
23. Ref. 21, pp. 137–138.
24. Ref. 21, p. 48.
25. Ref. 13, Chap. 8.
26. Ref. 21, Fig. 2.7.
27. A. J. Simpson and M. J. Fitter, “What is the best index of detectability?” *Psychol. Bull.* **80**, 481–488.
28. Ref. 21, pp. 67–70.
29. S. P. McKee and S. N. J. Watamaniuk, “The psychophysics of motion perception,” in *Visual Detection of Motion*, A. T. Smith and R. J. Snowden, eds. (Academic, New York, 1994), p. 85.
30. D. M. Levi, S. A. Klein, and P. Aitsebaomo, “Detection and discrimination of the direction of motion in central and peripheral vision or normal and amblyopic observers,” *Vision Res.* **24**, 789–800 (1984).
31. Ref. 21, pp. 221–223.
32. Ref. 14, Chap. 6 and Appendix B.
33. Ref. 13, p. 224.
34. R. C. Emerson, J. R. Bergen, and E. H. Adelson, “Directionally selective complex cells and the computation of motion energy in cat visual cortex,” *Vision Res.* **32**, 203–218 (1992).
35. P. Hammond, “Directional tuning of complex cells in area 17 of the feline visual cortex,” *J. Physiol.* **285**, 479–491 (1978).
36. J. R. Maunsell and D. C. van Essen, “Functional properties of neurons in middle temporal visual area of the macaque monkey. I. Selectivity for stimulus direction, speed, and orientation,” *J. Neurophysiol.* **49**, 1127–1147 (1983).
37. D. M. Green, “Detection of auditory sinusoids of uncertain frequency,” *J. Acoust. Soc. Am.* **33**, 897–903 (1961).
38. H. Urkowitz, “Energy detection of unknown deterministic signals,” *Proc. IEEE* **55**, 523–531 (1967).
39. W. B. Davenport and W. L. Root, *An Introduction to the Theory of Random Signals and Noise* (McGraw-Hill, Toronto, 1958).
40. D. J. Lasley and T. E. Cohn, “Why luminance discrimination may be better than detection,” *Vision Res.* **21**, 273–278 (1981).
41. D. G. Pelli, “Uncertainty explains many aspects of visual contrast detection and discrimination,” *J. Opt. Soc. Am. A* **2**, 1508–1532 (1985).